Robust entanglement with a thermal mechanical oscillator

Andrey A. Rakhubovsky* and Radim Filip
Department of Optics, Palacký University, 17. listopadu 1192/12, 771 46 Olomouc, Czech Republic
(Received 14 January 2015; published 15 June 2015)

We consider a protocol to entangle an electromagnetic pulse with a mechanical oscillator at high temperature. We show this protocol to be capable of entangling currently existing experimental systems at relatively high (above the available cryostat) temperatures of the mechanical part. We also predict a possibility of conditional squeezing of the mechanical mode below the shot noise level at the cryostat temperatures.

DOI: 10.1103/PhysRevA.91.062317 PACS number(s): 03.67.Bg, 42.50.Wk, 42.50.Ex, 42.50.Dv

I. INTRODUCTION

Quantum optomechanics is a rapidly developing field of quantum physics with continuous variables profiting from the new possibilities of quantum control of mechanical oscillators [1–4]. This hybrid experimental platform directly links the quantum properties of light and microwave radiation, represented by the model of a linear oscillator, with the characteristics of real mechanical-type oscillator. These quantum mechanical oscillators have physical features and capabilities that distinguish them from the properties of light, many times examined in details in continuous-variable quantum optics [5–7]. Mechanical vibration of the real position of the oscillator naturally allows the bridge to thermodynamics and recently ongoing examination of quantum thermodynamics with mechanical oscillators [8–10]. Thinking about this direction at a very basic level, we first admit that the mechanical oscillator is an open system. It naturally tends to thermodynamic equilibrium with its thermal environment. Second, quantum optomechanics can advantageously exploit radiation pressure to push the mechanical oscillators out of thermodynamic equilibrium and, therefore, it allows us to generate interesting quantum effects.

Continuous-variable quantum entanglement [5] is a basic phenomenon demonstrating the connection between light and mechanical oscillator out of thermal equilibrium. Theoretically, an interaction caused by radiation pressure allows the entangling process of amplification of mechanical vibration and radiation at the same time [2]. In quantum optics, such amplification processes in nonlinear crystals lead to the generation of squeezed states of light and Gaussian entanglement between optical beams [7]. These are useful resources for a variety of operations developed in quantum optics and quantum information processing [7,11,12]. In quantum optics, it is easy to achieve the ground state of the mode of light modeled by the linear harmonic oscillator since the light interacts very weakly with matter and the modes can be easily blocked. On the other hand, the mechanical oscillators are inherently thermally occupied by phonons and their cooling is necessary by use of sophisticated techniques [4]. For the intensively cooled electromechanical oscillators, Gaussian quantum entanglement has been recently experimentally demonstrated in the pulsed regime [13]. At the same time, it was theoretically predicted that Gaussian quantum entanglement is observable at the output of the amplification process for thermal-equilibrium input states with arbitrary temperature [14]. These methods could, in principle, generate *thermal* entanglement without any cooling mechanical oscillators and also the nonclassical squeezed state of the mechanical oscillator. Such thermal entanglement does not naturally occur in optical nonlinear processes, so this type of thermal Gaussian entanglement has not been studied in quantum optics. In pulsed quantum optomechanics it is possible to achieve an ideal amplification regime approximatively by an adiabatic elimination of the optical mode when the mechanical oscillator is not much thermally occupied [15–17]. Unfortunately, this approximation is generally not applicable for an interesting case of extreme temperature of the mechanical oscillator, where thermal entanglement can still be surprisingly detected.

In this paper, the pulsed generation of thermal entanglement between light and mechanical oscillator is analyzed without using the adiabatic approximation. The bound on generation of the entanglement is defined in the limit of the large temperature of the mechanical oscillator. Generation of thermal entanglement is analyzed for the current electromechanical experiment [13] and subsequently for the future optomechanical experiment [18]. For both types of experiments, existence and robustness of the thermal Gaussian entanglement is confirmed for the large number $n_{\mathrm{th}} \approx 400$ of thermal phonons for the experiment in [13] and $n_{\mathrm{th}} \approx 240$ for the experiment in [18]. In addition, it is shown that thermal entanglement allows

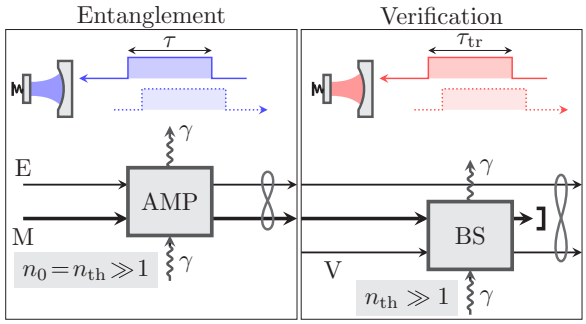

FIG. 1. (Color online) Protocol to create and verify entanglement. First the blue-detuned entangling pulse with length τ enters the cavity, then after the delay time τ_{del} the red-detuned pulse lasting τ_{tr} performs the read-out of the state of the mechanical subsystem. Mechanical system is initially in a thermal state with occupation n_0 and is coupled at the rate γ to the thermal bath with occupation n_{th}.

*andrey.rakhubovskiy@upol.cz

one to prepare nonclassical squeezed states of the mechanical oscillator in both proposed experiments. A temperature limit for the generation of the squeezed states is derived and compared to the temperature limit for the existence of thermal interconnection. Currently, all these conclusions can be directly tested in the electromechanical experiment [13] and they can speed up the observation of the optomechanical entanglement. The optomechanical entanglement is then more compatible with developed techniques of quantum optics.

II. MODEL OF SYSTEM

We consider a general optomechanical setup with the Hamiltonian [19],

$$H = \hbar\omega_c a^\dagger a + \hbar\omega b^\dagger b - \hbar g_0 a^\dagger a(b + b^\dagger) - \\ - i\hbar\mathcal{E}(a^\dagger e^{i\omega_p t} - a e^{-i\omega_p t}).$$

This Hamiltonian is peculiar to a wide variety of optomechanical devices including microwave resonators [13,20], optomechanical crystals [18,21], microresonators [22], setups with membrane inside a cavity [23,24] or whispering-gallery-mode resonators [25]. Physically this Hamiltonian corresponds to the two interacting modes: a single mode of a mechanical oscillator and a mode of the optical field in a pumped cavity.

The first two summands represent the Hamiltonians of the optical and the mechanical modes, respectively. The optical (mechanical) mode is characterized by frequency ω_c (ω) and the annihilation operator a (b). The third summand is the radiation pressure interaction Hamiltonian with the single-photon coupling constant denoted as g_0. The last term stands for pumping with the frequency $\omega_p = \omega_c - \Delta$. The parameter $\mathcal{E}$ is related to the input light power P_i as $|\mathcal{E}| = \sqrt{2\kappa P_i/\hbar\omega_p}$ where κ is the amplitude decay rate of the cavity.

In experiment the single-photon optomechanical coupling strength g_0 is typically very low so in order to enhance the interaction a strong classical pump is applied. The dynamics of the system is therefore linearized near a steady state [3,4,26]. The system of linearized Heisenberg-Langevin equations then reads

$$\begin{aligned} \dot{q} &= \omega p, \\ \dot{p} &= -\omega q - \gamma p + g_0\sqrt{2n_{\rm cav}}(a + a^\dagger) + \sqrt{2\gamma}\xi, \\ \dot{a} &= -(\kappa + i\Delta)a + i g_0\sqrt{2n_{\rm cav}}q + \sqrt{2\kappa}a^{\rm in}, \end{aligned} \tag{1}$$

with $q = (b^\dagger + b)/\sqrt{2}$ and $p = i(b^\dagger - b)/\sqrt{2}$ being dimensionless mechanical position and momentum quadratures. In the equations above γ is the mechanical viscous damping rate, and the coupling rate g_0 is enhanced by the average intracavity photon number $n_{\rm cav} = 2\kappa P_i/(\hbar\omega_c(\kappa^2 + \Delta^2))$.

The mechanical damping force $\sqrt{2\gamma}\xi$ is non-Markovian in general [27], however, it can be treated as Markovian if the following two conditions are met: (i) bath occupation number $n_{\rm th} = k_B T/\hbar\omega \gg 1$ is not too low and (ii) mechanical quality factor is high, $Q = \omega/\gamma \to \infty$. These conditions are well satisfied in the majority of contemporary experimental setups which makes valid the use of a standard Markovian correlation function:

$$\langle \xi(t) \circ \xi(t')\rangle \equiv \tfrac{1}{2}\langle \xi(t)\xi(t') + \xi(t')\xi(t)\rangle \\ \approx (n_{\rm th} + 1/2)\delta(t - t').$$

The optical Langevin force $a^{\rm in}$ represents the field incident to the cavity and is assumed to be in the vacuum state hence $\langle a^{\rm in}(t) \circ a^{\rm in\dagger}(t')\rangle = 1/2\,\delta(t - t')$. This is true for optical fields at room temperature or for microwaves at a cryostat.

Depending on detuning of the pump with respect to the cavity mode different types of interaction between the two modes prevail. In case of resonant red detuning (i.e., when the pump frequency is lower than the cavity one, $\Delta = \omega$) the *beamsplitter*-type interaction is dominant. This interaction is characterized by the Hamiltonian,

$$H_{\rm bs} = a^\dagger b + a b^\dagger, \tag{2}$$

and is capable of swapping the states between the interacting modes. This type of interaction was applied [18,20] to transfer the vacuum state of the field to the mechanical system in order to cool the latter.

In the opposite case of resonant blue detuning when the pump frequency is larger than the cavity mode frequency ($\Delta = -\omega$) the dominant interaction is the *amplification* or *two-mode squeezing* one with the Hamiltonian,

$$H_{\rm amp} = a^\dagger b^\dagger + a b. \tag{3}$$

Two-mode squeezing interaction is known for its ability to entangle the two interacting modes and was considered to create entanglement in an optomechanical system. However, due to instabilities accompanying this type of interaction the coupling strength is not sufficient to reach entanglement in continuous wave regime. To relax the stability requirement it was proposed by Hofer *et al.* [15] to implement a pulsed protocol employing amplification-type interaction (3) to entangle an optomechanical system. Recently, this interaction has been used [13] to generate entanglement in an electromechanical system.

III. ENTANGLING PROTOCOL

The protocol proposed to create and verify entanglement in an optomechanical system comprises interaction of two sequential time-separated pulses (see Fig. 1) with the mechanical oscillator. The first pulse is resonantly blue detuned and relies on the two-mode squeezing interaction (3) to create the optomechanical entanglement. The consequent pulse is red detuned and therefore utilizes the beam-splitter-type interaction (2) to verify the optomechanical entanglement by reading out the state of the mechanical mode.

The authors of Ref. [15] perform analysis of the entanglement (see brief summary in Appendix B) followed by general numerical simulations. The analytical consideration is based on the adiabatic elimination of the cavity mode which unfortunately results in overestimation of the optomechanical entanglement. This difference is especially important in the limit of large occupation numbers (higher temperatures).

For examination of the entanglement in Ref. [15] the inseparability criterion based on estimation of the symmetric EPR variance [28] was used. This method, however, can lead

TABLE I. Values of parameters used for numerical estimations.

Quantity	Palomaki *et al.* [13]	Chan *et al.* [18]
Mechanical frequency ω	$2\pi \times 10.34$ MHz	$2\pi \times 3.9$ GHz
Viscous damping rate γ	$2\pi \times 35$ Hz	$2\pi \times 39$ kHz
Cavity half width κ	$2\pi \times 180$ kHz	$2\pi \times 0.25$ GHz
Sideband resolution parameter κ/ω	0.02	0.06
Single-photon coupling g_0	$2\pi \times 200$ Hz	$2\pi \times 0.9$ MHz
Photon number $n_{\mathrm{cav;B}} = n_{\mathrm{cav;R}}$	24×10^3	1.5×10^3
Enhanced coupling $g_B = g_R$	$2\pi \times 30.9$ kHz	$2\pi \times 35.0$ MHz
Coupling $G_B = G_R = G_0$	$2\pi \times 5.3$ kHz	$2\pi \times 9.8$ MHz
Duration of entangling pulse τ	35 μs	0.13 μs
Time span between the pulses $\tau_{\mathrm{del}}^{(0)}$	10 μs	0.04 μs
Duration of the verification pulse τ_{tr}	10 τ	10 τ

to underestimation of entanglement in case the state being analyzed is asymmetric (i.e., variances of one of the modes are exceedingly higher than those of the another). According to the recent research [14] this is the very case of the optomechanical entanglement particularly at higher temperatures. To avoid this we use logarithmic negativity [29] as a measure of entanglement. For a brief review of the mentioned measures of entanglement we refer the reader to Appendix A.

Our analysis complements the results previously reported owing to several differences. First we carry out a complete numerical analysis of the system described by Eq. (1) with the only approximation of rotating wave (which is justified by good sideband resolution $\kappa/\omega \ll 1$ in the setups we consider; see Table I). In our calculations we do not use the adiabatic elimination of the cavity mode. Second, as a criterion for the presence of entanglement we use logarithmic negativity [29] instead of EPR variance [28]. Applying this distinctive feature we analyze to which extent the recent predictions of robust entanglement [14,17] in optomechanical systems are valid.

In the experiment [13] the pulsed protocol was realized in an electromechanical setup. The mechanical mode was pre-cooled using an additional red detuned pulse. The entanglement between the mechanics and field was then quantified by measuring the covariance matrix of quadratures of pulses leaking from the circuit. Below in comparison to the results of [13,15] we present analysis of the entanglement between these two pulses as well as the analysis of the entanglement between the mechanical mode and the entangling pulse.

IV. ESTIMATION OF COVARIANCE MATRIX

The linearized equations of motion for the system read in matrix form,

$$\dot{u}(t) = Au(t) + f(t),$$

where $u = (X,Y,q,p)$ is the vector of intracavity quadratures and $f = (\sqrt{2\kappa}X^{\mathrm{in}}, \sqrt{2\kappa}Y^{\mathrm{in}}, \sqrt{\gamma}\xi, \sqrt{\gamma}\xi)$ is the vector of Langevin forces; X,Y and $X^{\mathrm{in}}, Y^{\mathrm{in}}$ are the quadratures, respectively, of the intracavity field a and the Langevin force a^{in}. The form of the so-called drift matrix A peculiar to a particular type of interaction can be deduced from the general form [13,26],

$$A = \begin{pmatrix} -\kappa & 0 & g_B & g_R \\ 0 & -\kappa & -g_R & -g_B \\ g_B & g_R & -\gamma/2 & 0 \\ -g_R & -g_B & 0 & -\gamma/2 \end{pmatrix},$$

by equating $g_R = 0$ for the blue detuned pulse, $g_B = 0$ for the red detuned pulse or both $g_B = g_R = 0$ for the free evolution between the pulses ($g_{B,R}$ denote the optomechanical coupling enhanced by a number of intracavity photons in the corresponding pulse: $g_i = g_0\sqrt{n_{\mathrm{cav},k}}; k = B,R$).

The system under consideration is initially in a Gaussian state and the linear dynamics preserves this quality. So the correlation properties of the system can be completely characterized by its two first moments, of which we are interested in second ones, namely the covariance matrix (CM) with elements defined as

$$V_{ij}(t) = \langle u_i(t) \circ u_j(t) \rangle. \tag{4}$$

To estimate it we use the approach similar to the one of Refs. [30,31]. The solution of the equations of motion could be formally written in the form,

$$u(t) = M(t - t_0)u(t_0) + \int_{t_0}^{t} ds M(t - s) f(s), \tag{5}$$

where M is the matrix exponential $M(t) = \exp(At)$. Performing substitution of the equation above into the definition of elements of the CM and interchanging the order of integration and averaging one can obtain the expression for the covariance matrix of the intracavity quadratures:

$$V(t) = M(t - t_0)V(t_0)M^{\top}(t - t_0) + \int_{t_0}^{t} ds M(t - s) F M^{\top}(t - s),$$

where $^{\top}$ stands for transposition, F is a matrix of correlations between the Langevin forces:

$$\langle f_i(s) \circ f_j(s') \rangle \equiv F\delta(s - s') = \mathrm{diag}\left[\kappa, \kappa, \gamma\left(n_{\mathrm{th}} + \tfrac{1}{2}\right), \gamma\left(n_{\mathrm{th}} + \tfrac{1}{2}\right)\right]\delta(s - s').$$

In [13] the entanglement was authenticated by analysis of the covariance matrix between the quadratures of the entangling pulse and the verification pulse. These quantities following the considerations of [15] were defined by projection of the leaking field quadratures $u^{\rm out} = (X^{\rm out}, Y^{\rm out})$ on the exponential envelopes. Explicitly this projection reads

$$U^B = C_B \int_{T_B} dt u^{\rm out}(t) e^{G_B t}, \quad U^R = C_R \int_{T_R} dt u^{\rm out}(t) e^{-G_R t}. \tag{6}$$

The integration is done over the duration of corresponding pulse denoted as $T_{B,R}$; $C_{B,R}$ is the normalizing coefficient, so $[U_1^k, U_2^k] = i$, where $k = B, R$. The exponential rates are defined as $G_k = g_k^2/\kappa$.

The quadratures of the leaking field are computed using the usual input-output relations [32],

$$u_j^{\rm out}(t) = \sqrt{2\kappa}\, u_j(t) - u_j^{\rm in}(t), \quad j = 1,2. \tag{7}$$

Here $u^{\rm in} = (X^{\rm in}, Y^{\rm in})$ denotes the vector of quadratures of the input field. Please note that both $u^{\rm out}$ and $u^{\rm in}$ are two-dimensional vectors so only the first two components of u are used.

Using the definitions given one can make estimations for the covariance matrix of the quadratures of the two pulses. The matrix is written as follows with the help of 2×2 blocks that contain autocorrelations of and cross correlations between the two pulses,

$$\mathbb{V}_{\rm p} = \begin{pmatrix} \langle U_i^B \circ U_j^B \rangle & \langle U_i^B \circ U_j^R \rangle \\ \langle U_j^B \circ U_i^R \rangle & \langle U_i^R \circ U_j^R \rangle \end{pmatrix}, \quad i,j = 1,2.$$

To compute the elements of $\mathbb{V}_{\rm p}$ we use the same approach. We substitute the formal solution (5) and the definition of pulse quadratures (6) into the input-output relations (7). After swapping the order of the averaging over state and of the integration over time we are able to relate $\mathbb{V}_{\rm p}$ with the covariance matrix V_0 of the initial state of the system and the correlations of the Langevin forces.

In more details, for instance, for $\langle U_i^B \circ U_j^B \rangle$ one can obtain

$$\begin{aligned} \left\langle U_i^B \circ U_j^B \right\rangle = C_B^2 \int \int_{T_B} dt dt'\, e^{G_B(t+t')} \times 2\kappa \Big[& M(t) V_0 M^{\top}(t') \\ & + \int_0^t ds \int_0^{t'} ds' M(t-s) F \delta(s-s') M^{\top}(t'-s') \\ & - \int_0^t ds M(t-s) \widetilde{F}(s-t') \\ & - \int_0^{t'} ds' \widetilde{F}(s'-t) M^{\top}(t'-s') \\ & + \frac{1}{2\kappa} \widetilde{F}(t-t') \Big]_{ij}, \\ i,j = 1,2. & \end{aligned}$$

In this equation we introduced a new matrix $\widetilde{F}$ characterizing correlations between the intracavity Langevin forces (elements of f) and the quadratures of incident field $u^{\rm in}$, namely,

$$[\widetilde{F}(s-s')]_{ij} \equiv \left\langle u_i^{\rm in}(s) \circ u_j^{\rm in}(s') \right\rangle = {\rm diag}\left[\tfrac{1}{2}, \tfrac{1}{2}, 0, 0\right] \delta(s-s').$$

The mechanical subsystem is assumed to be initially in a thermal state with occupation number n_0, and the field inside the cavity is assumed to be in vacuum, so the covariance matrix of the initial state is as follows:

$$V_0 = {\rm diag}\left[\tfrac{1}{2}, \tfrac{1}{2}, n_0 + \tfrac{1}{2}, n_0 + \tfrac{1}{2}\right].$$

V. RESULTS OF COMPUTATION

A. Verification of entanglement

To prove the validity of our method we first compare the results we obtain with the experimental ones reported in Ref. [13], namely we estimate the covariance matrix of the two consequent pulses (the entangling and verification ones) for the same experimental setup.

The result of numerical analysis is presented in Fig. 2(a) (for the exact values of parameters we used for estimations please see Table I). The inset to the figure represents nonzero elements of the covariance matrix of the quadratures of two pulses for a pre-cooled close to the ground-state mechanical oscillator in a cryogenic bath ($n_0 = 0$, $n_{\rm th} = 40$). Empty bars correspond to the elements obtained in the case of perfect detection ($\eta = 1$) and solid bars correspond to attenuation in both modes $\eta = 0.2$. We see here a good quantitative coincidence with the reported experimental results.

The figure contains two pairs of traces of logarithmic negativity between the two pulses versus the mechanical occupation. The initial occupation n_0 of the mechanical mode along the traces is assumed to be equal to the occupation $n_{\rm th}$ of the mechanical bath (the mechanical mode is assumed to be at equilibrium state with its environment).

The darker curves employ the parameters reported in Ref. [13]. The logarithmic negativity is computed under the assumption of perfect detectors and absence of losses (dashed line) and under the realistic assumption of damping in both modes with effective transmittance $\eta = 0.2$ (solid line) due to nonperfect detection.

It is clear from the figure that the entanglement between the pulses is robust against temperature of the mechanical environment which proves the pre-cooling stage is unnecessary in the entangling protocol (the maximum temperature allowing entanglement is $\sim$65 mK, about three times higher than the temperature of the cryostat). Comparison of the traces demonstrates that the damping in both modes does not completely destroy the entanglement but only decreases its value, i.e., the entanglement is robust against attenuation in both modes. It is a clear witness that the robust version of thermal entanglement predicted in [14] can be observed in recent experiment [13].

The two steeper (lighter) curves in Fig. 2(a) represent logarithmic negativity computed for the same protocol within the optomechanical crystal experimental setup reported in Ref. [18]. Although the phonon number boundary is lower in this case, one should note that the frequency of the mechanical mode is several orders higher in this experiment and owing to this the boundary temperature is actually higher (more than 40 K, twice as high as the temperature of the corresponding cryostat, 20 K).

It needs to be underlined that the negativity estimated in Fig. 2(a) is the measure of entanglement between the two

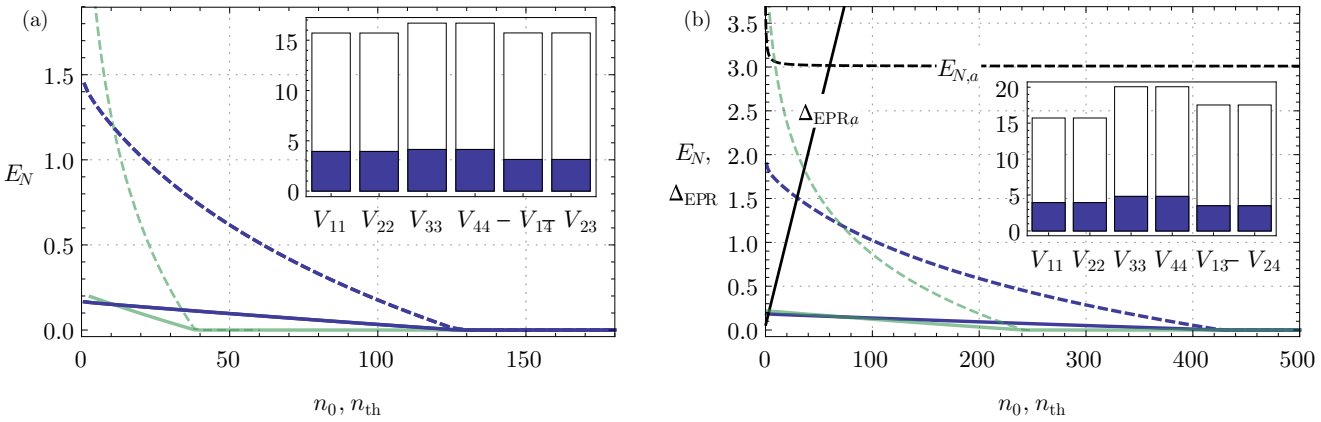

FIG. 2. (Color online) Different types of entanglement (logarithmic negativity) versus the temperature (occupation number) of the mechanical subsystem. (a) Entanglement between the quadratures of the entangling and the verification pulses. (b) Entanglement between the entangling pulse and the mechanical mode. Darker (blue) traces, electromechanical experimental setup reported by Palomaki *et al.* [13]; lighter (green) traces, optomechanical crystal by Chan *et al.* [18]. Dashed lines, lossless case; solid lines, realistic damping in both modes, $\eta = 0.2$. (Inset) Nonzero elements of covariance matrix simulating the experiment from Ref. [13] (initial mechanical occupation $n_0 = 0$, mechanical bath occupation $n_{\rm th} \approx 40$). Black lines in (b) represent logarithmic negativity $E_{N,a}$ and EPR variance $\Delta_{{\rm EPR},a}$ of the optomechanical system calculated after the adiabatic elimination of the cavity mode. For the parameters utilized for estimations see Table I.

pulses emerging from the cavity but not between field and matter although the entanglement is created by means of optomechanical interaction.

It is also illustrative to check how the entanglement between the pulses can tolerate longer separations between the pulses. The dependence of the logaritmic negativity on the time separation of the pulses (in units of $\tau_{\rm del}^{(0)}$ used to plot Fig. 2) is presented in Fig. 3. It shows, for instance, that the entanglement between the two pulses can persist even when the time span between them is twice as long as the duration of the entangling pulse.

B. Optomechanical entanglement

Another figure of merit is the optomechanical entanglement between the motion of the mechanical subsystem and the quadratures of the leaking field immediately after the entangling pulse. This entanglement exhibits even stronger robustness against the noisy thermal bath of the mechanical mode. The traces of logarithmic negativity versus the mechanical occupation are presented in Fig. 2(b).

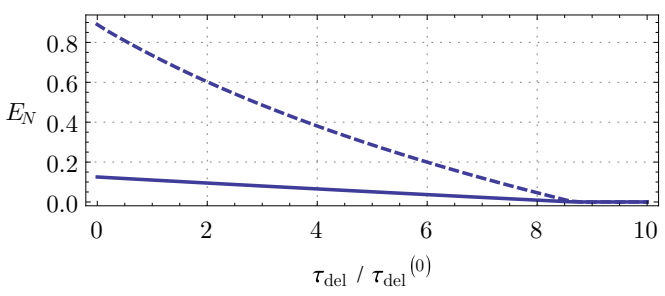

FIG. 3. (Color online) Dependence of the entanglement between the two pulses on the time span between them for the parameters of experiment by Palomaki *et al.* [13]. Dashed and solid lines correspond to the lossless case and the case of losses $\eta = 0.2$, respectively.

The two pairs of lighter curves represent the logarithmic negativity estimated using our approach versus the mechanical occupation for Refs. [13] and [18]. The optomechanical entanglement in this setup appears to be robust to both the temperature of the mechanical bath and the initial temperature of mechanical mode as well as robust to attenuation in both mechanical and optical modes.

In the inset to Fig. 2(b) one can see the visualization of nonzero elements of the covariance matrix between the blue pulse and the mechanical mode after the (entangling) interaction is complete. Comparison of this covariance matrix with one of the two pulses reveals that the verification (red detuned) pulse does indeed perform state transfer from the mechanical mode to the leaking field with efficiency close to the ratio $\kappa_{\rm ext}/\kappa$ of two decay rates: the one due to the coupling of the circuit to the transmission line and the total decay rate of the circuit. The residual discrepancy is caused by the mechanical decoherence taking place during the interval between the pulses.

Due to the nonzero temperature of the mechanical bath ($n_{\rm th} \neq 0$) the optomechanical state is asymmetrical even though the initial occupation of the mechanical mode was equal to zero ($n_0 = 0$). The asymmetry grows with an increase of $n_{\rm th}$ as it was predicted in [14].

In Fig. 2(b) we also compare the results of our computations with the predictions made after the adiabatic elimination of the cavity mode. On one hand the bound for $n_0 = n_{\rm th}$ allowing entanglement predicted by $\Delta_{\rm EPR}$ for an electromechanical system [13] ($n_{0;{\rm th}} \sim 50$, $T \sim 25$ mK) is significantly lower than by logarithmic negativity ($n_{0;{\rm th}} > 400$, $T > 0.2$ K). On the other hand, if one estimates the logarithmic negativity for the system after adiabatic elimination, this entanglement appears to exist at arbitrary occupations (see dashed black line in Fig. 2(b)). According to the principal considerations in [14] this is possible in blue detuning if the interaction is strong enough which is the case in the pulsed systems.

C. Squeezing of the mechanical mode

One more promising application of the entangling protocol is the possibility of conditional squeezing of the mechanical subsystem state. After the entangling pulse leaves the cavity the quadratures of the former are strongly correlated with the quadratures of the mechanical mode. Therefore the measurement (or a proper postselection) on the optical side is able to project the mechanical mode into a squeezed state.

Our analysis shows that after a measurement performed on an *arbitrary* combination of the quadratures of the blue pulse $X_\theta^L = U_1^B \cos\theta + U_2^B \sin\theta$ some quadrature of the mechanical mode $X_\phi^M = q\cos\phi + p\sin\phi$ is squeezed, i.e., has variance under the shot-noise level (1/2 in our notation).

The effect is more pronounced in lower temperatures where an arbitrarily weak coupling can create the correlations capable of consequent conditional squeezing. With an increase in the temperature (mechanical occupation) the boundary for coupling appears. The dependence of this effect on the temperature of the bath and the coupling strength is illustrated in Fig. 4. The solid line depicts dependency of the minimal mechanical variance on the temperature for a fixed coupling strength.

The solid and dashed lines represent the lowest coupling strength necessary to achieve, respectively, entanglement (ζ_e) and the possibility of conditionally squeezing the mechanical mode (ζ_m). These coupling strengths are normalized $\zeta = G/G_0$; the normalization factor G_0 is the coupling strength utilized for Figs. 2(a) and 2(b).

According to the numerical estimations, for a fixed coupling strength there is a region of temperatures that allows the creation of entanglement but not the conditional squeezing of the mechanical mode. This is not inherent in the adiabatic elimination case, as well as in [14], where (in both cases) the interaction between the two modes is represented purely by amplification (3). In the latter case once the coupling is strong enough to allow conditional squeezing this possibility persists for the arbitrary phonon number.

Conditional squeezing is robust to arbitrary attenuation in the mechanical mode, and is to some extent robust to attenuation of the entangling pulse; the latter robustness increases with an increase of the coupling strength.

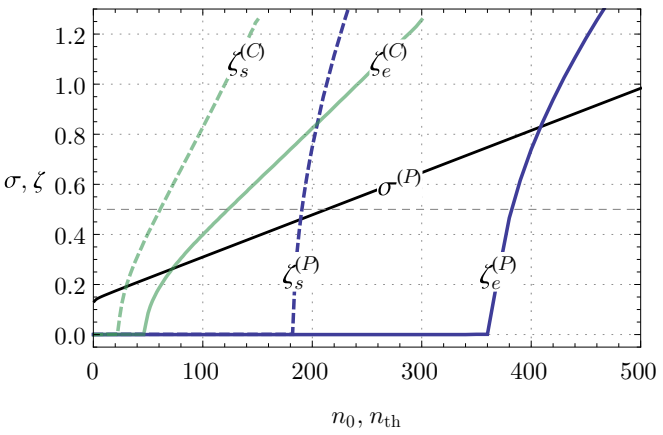

FIG. 4. (Color online) Minimal coupling (in relative units) allowing conditional squeezing ζ_s and entanglement ζ_e for parameters of experiment by Palomaki *et al.* [13] ($\zeta^{(P)}$) and by Chan *et al.* [18] ($\zeta^{(C)}$). (Solid line) Minimal variance σ of the conditional mechanical state versus mechanical occupation (parameters from [13]). The conditional squeezing is possible if $\sigma < 1/2$.

VI. CONCLUSION

We consider a pulsed optomechanical setup to generate the entanglement and address the question of whether this is possible at relatively high temperatures. The original paper by Hofer *et al.* [15] proposing the pulsed entangling protocol provides estimations of the upper boundary for the temperature that allows entanglement. We are able to amend these estimations by a complete numerical analysis of the system for the high temperature limit where [15] cannot be used.

The distinctions of our approach are (i) we take into account the full system of Heisenberg-Langevin equations of motion (1) and (ii) we use a measure of entanglement which allows us to see also the entanglement of asymmetric states—such as the optomechanical states at higher temperatures.

We analyze the optomechanical entanglement between the mechanical mode and the leaking field as well as the optical entanglement of the entangling and the verification pulses. Our numerical results for the latter coincide with the experimental data reported in Ref. [13]. According to our estimations it is possible to create entanglement in currently achievable experimental conditions at cryostat temperatures that were already experimentally reported in [13,18].

Finally we demonstrate that the entangling protocol is capable of conditional squeezing of the very noisy mechanical mode, i.e., the interaction with a pulse provides the possibility of projecting the mechanical mode to a state with the variance of one of the quadratures below the shot noise level by means of measurement performed on the optical mode. We show that this effect is robust to temperatures as well as the entanglement.

The existence and robustness of thermal optomechanical and electromechanical entanglement is a prerequisite for future advanced methods, where the thermal mechanical oscillator can mediate an interaction between other physical systems. As an example, it was already proposed that the thermal mechanical oscillator is tolerable during a generation of entanglement between two microwave fields [33].

ACKNOWLEDGMENTS

We are thankful to Sebastian Hofer for stimulating discussions. A.R. acknowledges financial support from Grant No. P205/12/0694 of the Czech Science Foundation. R.F. acknowledges financial support from Grant No. GA14-36681G of the Czech Science Foundation.

APPENDIX A: ENTANGLEMENT MEASURES

In this Appendix we outline the properties of the two entanglement measures we use: logarithmic negativity and EPR variance.

Let us consider a system comprising two modes with position and momentum quadratures $u = (X, Y, q, p)$ satisfying commutation relations $[X, Y] = i$ and $[q, p] = i$. If such a system is in a zero-mean Gaussian state, the state can be completely described by a matrix of the second-order moments of the quadratures (covariance matrix) V defined by Eq. (4).

The covariance matrix is conveniently divided into blocks describing the two separate subsystems and the correlations between them:

$$V = \begin{pmatrix} V_{\mathrm{L}} & V_{\mathrm{c}} \\ V_{\mathrm{c}}^{\top} & V_{\mathrm{M}} \end{pmatrix},$$

where the blocks are

$$V_{\mathrm{L}} = \begin{pmatrix} \langle X^2 \rangle & \langle X \circ Y \rangle \\ \langle X \circ Y \rangle & \langle P^2 \rangle \end{pmatrix},$$

$$V_{\mathrm{M}} = \begin{pmatrix} \langle q^2 \rangle & \langle q \circ p \rangle \\ \langle q \circ p \rangle & \langle p^2 \rangle \end{pmatrix},$$

$$V_{\mathrm{c}} = \begin{pmatrix} \langle X \circ q \rangle & \langle X \circ p \rangle \\ \langle Y \circ q \rangle & \langle Y \circ p \rangle \end{pmatrix}.$$

The logarithmic negativity E_N of the state with covariance matrix V is then

$$E_N = \max\left[0, -\tfrac{1}{2}\log 2\left(\Sigma_V - \sqrt{\Sigma_V^2 - 4\det V}\right)\right],$$

where $\Sigma_V = \det V_{\mathrm{L}} + \det V_{\mathrm{M}} - 2\det V_{\mathrm{c}}$.

The state is entangled if and only if E_N is positive.

Another measure of entanglement is so-called EPR variance, introduced in Ref. [28]. The sufficient criterion for a state with covariance matrix V to be entangled is

$$\Delta_{\mathrm{EPR}} = \Delta[(X+p)^2] + \Delta[(Y+q)^2] < 2.$$

This condition is, however, not necessary for entanglement.

APPENDIX B: ENTANGLEMENT AFTER ADIABATIC ELIMINATION

In this Appendix we summarize the analysis of the dynamics under assumption of adiabatic elimination originally reported in Ref. [15].

Starting from the equations for the annihilation operators of the cavity (a) and the mechanical (b) modes describing the interaction with the entangling pulse,

$$\dot{a} = -\kappa a + igb^{\dagger} + \sqrt{2\kappa}a^{\mathrm{in}}, \quad \dot{b} = iga^{\dagger},$$

one can assume in the limit $g \ll \kappa \ll \omega$ that the optical mode reads out any changes in the mechanical motion almost instantaneously and hence adiabatically eliminate the cavity mode, setting $\dot{a} = 0$. Then the solution of these equations is substituted into the standard input-output relations [32] for the cavity $a^{\mathrm{out}} = -a^{\mathrm{in}} + \sqrt{2\kappa}a$ and input-output relations for new modes are written:

$$\begin{aligned} A_{\mathrm{out}} &= \sqrt{T}A_{\mathrm{in}} - i\sqrt{T-1}B_{\mathrm{in}}^{\dagger}, \\ B_{\mathrm{out}} &= \sqrt{T}B_{\mathrm{in}} - i\sqrt{T-1}A_{\mathrm{in}}^{\dagger}, \end{aligned} \tag{B1}$$

with $T = e^{2G\tau}$, $G = g^2/\kappa$, $B_{\mathrm{in}} = b(0)$, $B_{\mathrm{out}} = b(\tau)$, and the new optical input and output modes defined as

$$A_{\mathrm{in}} = \sqrt{\frac{2G}{1-e^{-2G\tau}}}\int_0^{\tau} dt e^{-Gt}a^{\mathrm{in}}(t),$$

$$A_{\mathrm{out}} = \sqrt{\frac{2G}{e^{2G\tau}-1}}\int_0^{\tau} dt e^{Gt}a^{\mathrm{out}}(t).$$

According to Eq. (B1) the output state of the optomechanical system is a two-mode squeezed state and one can apply the results of analysis done in Ref. [14] to it. In particular it was shown that the logarithmic negativity of a two-mode squeezed state of such a system is always positive (regardless of the initial occupation of the mechanical mode) if the interaction gain T exceeds 1, which means that the output state described by Eq. (B1) is always entangled.

Performing similar considerations for the verification pulse one can demonstrate that after the adiabatic elimination of the cavity mode interaction of the pulse with the mechanical mode is effectively a beam-splitter-type one.

[1] T. J. Kippenberg and K. J. Vahala, Opt. Express **15**, 17172 (2007).

[2] M. Aspelmeyer, S. Gröblacher, K. Hammerer, and N. Kiesel, J. Opt. Soc. Am. B **27**, A189 (2010).

[3] Y. Chen, J. Phys. B **46**, 104001 (2013).

[4] M. Aspelmeyer, T. J. Kippenberg, and F. Marquardt, editors, *Cavity Optomechanics* (Springer, Berlin, 2014).

[5] S. Braunstein and P. van Loock, Rev. Mod. Phys. **77**, 513 (2005).

[6] N. J. Cerf, G. Leuchs, and E. S. Polzik, (eds.), *Quantum Information with Continuous Variables of Atoms and Light* (Imperial College Press, London, 2007).

[7] A. Furusawa and P. v. Loock, *Quantum Teleportation and Entanglement* (John Wiley & Sons, New York, 2011).

[8] C. Elouard, M. Richard, and A. Auffèves, arXiv:1309.5276.

[9] A. Mari, A. Farace, and V. Giovannetti, arXiv:1407.8364.

[10] M. Brunelli, A. Xuereb, A. Ferraro, G. De Chiara, N. Kiesel, and M. Paternostro, arXiv:1412.4803.

[11] L. S. Madsen, V. C. Usenko, M. Lassen, R. Filip, and U. L. Andersen, Nat. Commun. **3**, 1083 (2012).

[12] S. Yokoyama, R. Ukai, S. C. Armstrong, C. Sornphiphatphong, T. Kaji, S. Suzuki, J.-i. Yoshikawa, H. Yonezawa, N. C. Menicucci, and A. Furusawa, Nat. Photonics **7**, 982 (2013).

[13] T. A. Palomaki, J. D. Teufel, R. W. Simmonds, and K. W. Lehnert, Science **342**, 710 (2013).

[14] R. Filip and V. Kupčík, Phys. Rev. A **87**, 062323 (2013).

[15] S. G. Hofer, W. Wieczorek, M. Aspelmeyer, and K. Hammerer, Phys. Rev. A **84**, 052327 (2011).

[16] Q. Y. He and M. D. Reid, Phys. Rev. A **88**, 052121 (2013).

[17] S. Kiesewetter, Q. Y. He, P. D. Drummond, and M. D. Reid, Phys. Rev. A **90**, 043805 (2014).

[18] J. Chan, T. P. M. Alegre, A. H. Safavi-Naeini, J. T. Hill, A. Krause, S. Groeblacher, M. Aspelmeyer, and O. Painter, Nature (London) **478**, 89 (2011).

[19] C. K. Law, Phys. Rev. A **51**, 2537 (1995).

[20] J. D. Teufel, T. Donner, D. Li, J. W. Harlow, M. S. Allman, K. Cicak, A. J. Sirois, J. D. Whittaker, K. W. Lehnert, and R. W. Simmonds, Nature (London) **475**, 359 (2011).

[21] S. M. Meenehan, J. D. Cohen, S. Gröblacher, J. T. Hill, A. H. Safavi-Naeini, M. Aspelmeyer, and O. Painter, Phys. Rev. A **90**, 011803 (2014).
[22] O. Arcizet, P.-F. Cohadon, T. Briant, M. Pinard, and A. Heidmann, Nature (London) **444**, 71 (2006).
[23] J. D. Thompson, B. M. Zwickl, A. M. Jayich, F. Marquardt, S. M. Girvin, and J. G. E. Harris, Nature (London) **452**, 72 (2008).
[24] D. Lee, M. Underwood, D. Mason, A. B. Shkarin, K. Borkje, S. M. Girvin, and J. G. E. Harris, arXiv:1406.7254.
[25] E. Verhagen, S. Deléglise, S. Weis, A. Schliesser, and T. J. Kippenberg, Nature (London) **482**, 63 (2012).
[26] C. Genes, A. Mari, D. Vitali, and P. Tombesi, in *Advances in Atomic, Molecular, and Optical Physics*, Vol. 57, edited by Ennio Arimondo, Paul R. Berman, and C. C. Lin (Academic Press, San Diego, 2009), pp. 33–86.
[27] V. Giovannetti and D. Vitali, Phys. Rev. A **63**, 023812 (2001).
[28] L.-M. Duan, G. Giedke, J. I. Cirac, and P. Zoller Phys. Rev. Lett. **84**, 2722 (2000).
[29] M. B. Plenio, Phys. Rev. Lett. **95**, 090503 (2005).
[30] J. Herec, J. Fiurášek, and L. Mišta Jr, J. Opt. B: Quantum Semiclassical Opt. **5**, 419 (2003).
[31] M. Paternostro, D. Vitali, S. Gigan, M. S. Kim, C. Brukner, J. Eisert, and M. Aspelmeyer, Phys. Rev. Lett. **99**, 250401 (2007).
[32] C. Gardiner and P. Zoller, *Quantum Noise: A Handbook of Markovian and Non-Markovian Quantum Stochastic Methods with Applications to Quantum Optics* (Springer Science & Business Media, Medford, 2004).
[33] L. Tian, Phys. Rev. Lett. **110**, 233602 (2013).